Eur J Anat, 15 (1): 17-28 (2011)

Anatomical bases of supraventricular arrhythmias

Damián Sánchez-Quintana, Margarita Murillo

Departamento de Anatomía y Biología Celular, Facultad de Medicina de Badajoz, Universidad de Extremadura, Avenida de Elvas s/n, 06006 Badajoz, Spain

SUMMARY

The adoption of catheter ablation techniques for the treatment of tachyarrhythmias in humans has increased the interest in cardiac anatomy. Interventional arrhythmologists have had to study the gross morphologic and architectural features of the heart. In addition, a new investigational wave has emerged to revisit cardiac anatomic topics for which the information was incomplete or simply wrong. As a result, recent studies have unraveled anatomic features, architectural aspects, and histologic details of certain components of the heart that are of interest to understand the substrates of tachycardias and their ablation. The purpose of this study was to review the gross morphological band structural details of the right and left atria such as the terminal crest (crista terminalis), cavotricuspid isthmus, Koch´s triangle, and its content, the Eustachian ridge or valve, the sub-Thebesian recess, the PV orifices and their neighboring left atrial landmarks and the architecture of the venoatrial junction. In addition, we describe the anatomy of the left atrial isthmus and, the oblique vein of Marshall. The relationship of the important structures in the neighborhood of the left atrium and the pulmonary veins as the oesophagus and phrenic nerves are also described.

Key words: Right atrium - Terminal crest - Cavotricuspid isthmus - Pulmonary veins - Oesophagus - Phrenic nerves

INTRODUCTION

Catheter ablation of cardiac arrhythmias has rapidly evolved from a highly experimental procedure to a standard form of therapy for several tachyarrhythmias, surpassing pharmacological treatments and surgical methods. Advances in this field have included (a) the development of techniques of catheter ablation, which often requires the precise destruction of minute amounts of arrhythmogenic tissues and (b) techniques of resynchronization therapy, which require pacing different parts of the atria as well as the ventricular branches of the coronary venous system. Preprocedural knowledge about cardiac anatomy can save time and improve the success rate and safety of the procedure by helping the electrophysiologist to choose the best region to perform the ablation. Localization of the anatomic structures of the atria before ablation is usually per-

Submitted: December 20, 2010
Accepted: January 18, 2011

Corresponding author:
Prof. Damián Sánchez-Quintana. Departamento de Anatomía y Biología Celular, Facultad de Medicina de Badajoz, Universidad de Extremadura, Avenida de Elvas s/n, 06006 Badajoz, Spain. Phone: 924-289434. E-mail: dasaqui55@yahoo.com; damians@unex.es

formed by fluoroscopy, electroanatomic mapping, and intracardiac echocardiography. With recent technological advances in multidetector CT scanners it has been possible to perform a "virtual dissection" of the heart and cardiovascular system.

Catheter-based ablation is usually preceded by a diagnostic electrophysiology study (EPS). A diagnostic EPS involves fluoroscopy-guided insertion of multiple catheters via the venous or arterial system to study and record the electrical activity from the atria, ventricles, and other specific parts of the conduction system, as well as to induce different types of arrhythmias to the underlying mechanism. AV conduction is studied by positioning a separate catheter across the tricuspid annulus and recording a His bundle electrogram. Radiofrequency (RF) current is the most commonly used energy source for cardiac ablation, delivering thermal energy to destroy the tissue (coagulative necrosis and oedema). Typical RF lesions are small, usually 3-6 mm in diameter and up to 3 mm deep when a standard catheter tip is used. Other energy sources that can be used include lasers, microwave, and ultrasound. The success of catheter ablation varies depending on the type of arrhythmia and the clinical situation. High success (>90%) rates and few complications (<3%) are seen in ablation procedures for arrhythmias such as atrioventricular nodal reentry, accessory pathways, atrial flutter, idiopathic ventricular tachycardia, and atrioventricular node or junction ablation. Lower success rates (<90%) and more complications (>3%) are seen in ablation procedures for atrial fibrillation, and postinfarction ventricular tachycardia.

The Cardiac Conduction System

The cardiac conduction system consists of the sinoatrial node (SAN), the atrioventricular node (AVN), the penetrating AV bundle (His bundle), the right and left bundle branches, as well as the fascicles and the Purkinje fibers (Fig. 1A). The conduction system is composed of specialized myocytes. Its atrial components, the SAN (subepicardial) and the AVN (subendocardial), are in contact with the atrial myocardium (Sánchez-Quintana and Ho, 2003, Malouf et al., 2004). While no morphologically distinct conduction pathway between the SAN and AVN is demonstrable, functional pathways due to the geometric arrangement of working muscle fibers could be responsible for conduction between the two structures along certain preferential routes (Malouf et al., 2004, Ho et al., 2002).The His bundle penetrates the right fibrous trigone (central fibrous body) and runs at the junction of the membranous septum and muscular septum before dividing into the right and left ventricular bundle branches (Sánchez-Quintana and Ho, 2003). The His bundle measures 12 cm in length. The right bundle branch is a cord-like structure approximately 5 cm in length and 1 mm in diameter runs along the septal and moderator bands to reach the anterior papillary muscle. The left bundle branch, in contrast, forms a broad sheet of conduction fibres divides along the left side of the interventricular septum into three indistinct fascicles (Sánchez-Quintana and Ho, 2003).

The Right Atrium (RA)

1. *Crista Terminalis (Terminal Crest)*

The RA is the anatomic gateway to the left atrium and a thorough understanding of its anatomy and anatomic variants is essential. The RA has three components; the appendage, the venous part, and the vestibule (Anderson and Brown, 1996). The crista terminalis (CT) (Fig. 1B) is a large muscular ridge that separates the smooth-walled venous part (sinus venarum) from the trabeculated appendage. The right atrial appendage is large and contains multiple pectinate muscles. The sinus venarum is located posterolaterally and receives the systemic [from the superior vena cava (SVC) and inferior vena cava (IVC)] and coronary (via the coronary sinus and small Thebesian veins) venous return. The right atrial vestibule is a smooth muscular wall around the tricuspid orifice, and supports the leaflets of the tricuspid valve. The characteristic feature of the vestibule is that it is surrounded by the pectinate muscles of the right atrium. The crista terminalis is a C shaped ridge of muscle formed by the junction of the sinus venosus and the primitive right atrium (Sánchez-Quintana et al., 2002, Matsuyama et al., 2004). The CT extends from the anteromedial wall on the left side of the entrance of the SVC (Fig. 1B), passes to the right in front of the venous orifice before descending laterally, curving to the right of the entrance of the IVC, to continue as an array of finer bundles that enter the region of the atrial wall recog-

Figure 1. **A**: Diagrammatic representation of the cardiac conduction system (in green) and the activation sequence on a surface electrocardiogram. The penetrating bundle perforates the insulating tissue plane of the atrioventricular (AV) junction to become the only bridge of muscular continuity between the atrial and ventricular myocardium. A=sinoatrial. **B**: Transillumination of the right atrium and fibromuscular membrane of the fossa ovalis (FO). Note the beginning of the terminal crest (TC) (dashed white line) over the limb of the fossa ovalis and surrounding the orifice of the superior vena cava (SVC). **C**: Sagittal histological section of the sinus node stained with haematoxylin-eosin. The node has been marked with a dashed black line. Note direct contact of this sinus node with the working cardiac cells of the crista terminalis. **D**: Schematic drawing showing the course of the artery to the AV node through the inferior pyramidal space and toward the central fibrous body. When viewed from the right atrial cavity, the triangle of Koch overlies the inferior pyramidal space. The AV node and conduction bundle are in yellow. CSO: Coronary Sinus Orifice; STV: Septal leaflet Tricuspid Valve; RAA: Right Atrial Appendage.

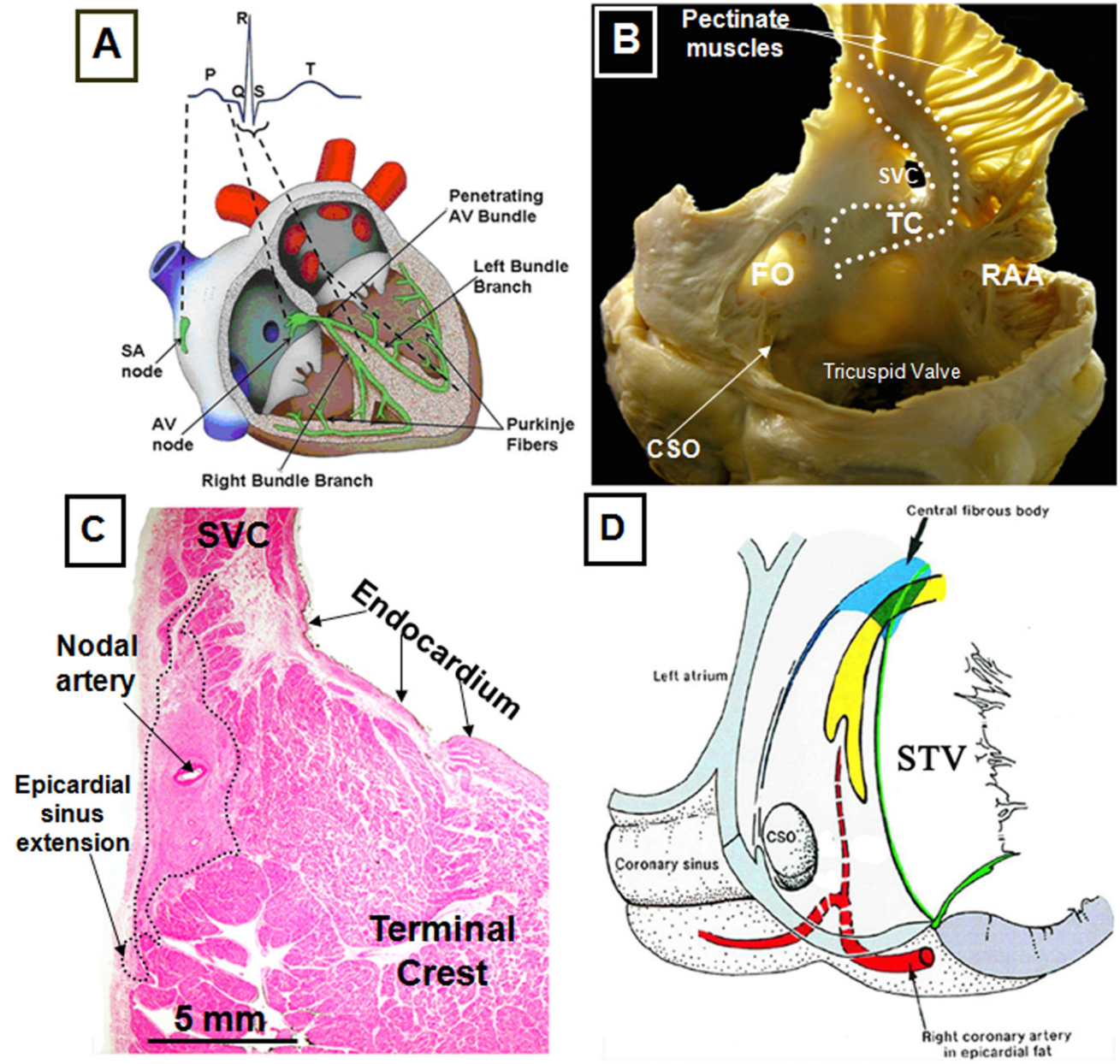

nized as the inferior isthmus or cavotricuspid isthmus. From the lateral margin of the crest arises a series of muscle bundles known as the pectinate muscles, which fan out from the crest toward the vestibular portion. The CT is a significant structure in several forms of atrial tachyarrhyhmias and, occasionally, it is the target for RF catheter procedures (Mizumaki et al., 2002). Ithas been suggested that the thickness of the crista terminalis may lead to the development of typical atrial flutter (Mizumaki et al., 2002).

The sinoatrial (SA) node is the source of the cardiac impulse. Histologically, it is composed of cells slightly smaller than normal working cells (Anderson et al., 1979, Chiu et al., 1989, Sánchez-Quintana et al., 2005a). The SA is a subepicardial spindle-shaped structure (Fig. 1C) at the superior cavoatrial junction that extends from the SVC along the crista termi-

nalis towards the IVC (Sánchez-Quintana et al., 2005a). It gradually penetrates the musculature of the crest to rest in the subendocardium. The SAN varies in position and length along the crista terminalis. The mean length of the SAN is has been reported to be 20 ± 3 mm (Matsuyama et al., 2004). Sinus cells are characterized by being clearer and embedded in a dense connective tissue matrix. With age, the amount of connective tissue increases with respect to the area occupied by the nodal cells (Inoue et al., 1986) in the periphery of the node, the specialized cells are mixed with those of the working myocardium. In addition, multiple radiations or extensions (Fig. 1C) interdigitating with the working atrial myocardium have been described. These penetrate intramyocardially into the crest, epicardium and the SVC (Sánchez-Quintana et al., 2005a). In axial CT images the SAN can be localized by locating the SA node artery along the crista terminalis. Modification of the sinus node using RF has been established as a treatment for inappropriate sinus tachycardia (Man et al., 2000). Because of the subepicardial location of the SA node, approaching from the endocardial surface requires more RF energy to ablate the sinus node (Sánchez-Quintana et al., 2002). MDCT can be used to measure the thickness of the crest and demonstrate the approximate location of the SAN artery within the nodal tissue. The centrally located nodal artery (Fig. 1C) may provide a cooling effect, reducing radiofrequency damage (Sánchez-Quintana et al., 2002, Sánchez-Quintana et al., 2005a, Man et al., 2000). The SAN artery is usually a single branch arising from the proximal right coronary artery (RCA) (60%) or left circumflex (LCx) artery (40%) (Anderson et al., 1979).

2. *Koch's Triangle*

Another area of the right atrium of significance to electrophysiologists is the triangle of Koch (Fig. 1D). This triangle is bordered posteriorly by a fibrous extension from the Eustachian valve called the tendon of Todaro (Ho and Anderson, 2000). The anterior border is demarcated by the attachment of the septal leaflet of the tricuspid valve. The apex of this triangle corresponds to the central fibrous body (CFB) of the heart where the His bundle penetrates. The so called 'fast pathway' corresponds to the area of musculature close to the apex of the triangle of Koch, the anatomic location of the atrioventricular node (AVN) (Fig. 1D). The base of the triangle is the orifice of the coronary sinus, and the vestibule of the right atrium immediately anterior to it. This part of the vestibule confined between the orifice of the coronary sinus and the attachment of the septal leaflet of the tricuspid valve, often referred to as the septal isthmus, is the area often targeted for ablation of the 'slow pathway' in AVNRT (Anderson et al., 2000). It is also the target for ablation of isthmus-dependent atrial flutter. The dimensions of Koch's triangle vary from one individual to another, which is clinically relevant in the case of catheter ablation procedures in this area, which are largely guided by anatomic landmarks.

The AV Node (AVN)is found at the apex of Koch's triangle. The AVN consists of a compact portion and an area of transitional cells (Anderson et al., 2000). The compact portion lies over the CFB (Fig. 2A). The size of the transitional cells is intermediate between those of the AV node and the atrial working cells. They are surrounded by a greater quantity of connective cells than that covering the working cells, but they are not insulated from the adjacent myocardium. Instead, they form a kind of bridge between the working and nodal myocardium, and collect electrical information from the atrial walls, transmitting it to the AV node. The AV node continues distally with the His bundle. The penetrating His bundle can readily be distinguished from the compact node at the point where the conduction axis itself becomes completely surrounded by tissues of the central fibrous body (Fig. 2B) and conducts electrical pulses to the ventricles (Anderson et al., 2000). The transition from the AV node to the His bundle is close to the apex of the triangle of Koch. The AVN artery originates from the apex of the U-turn of the distal right coronary artery (RCA) (Fig. 2C) and penetrates into the base of the posterior interatrial septum (inferior pyramidal space) at the level of crux of the heart in 80-87% of patients (Jazayeri et al., 1992, Sánchez-Quintana et al., 2001). In the remaining percentage of patients, it originates from the terminal portion of the LCx artery (8-13%) or, uncommonly, from both the RCA and the LCx (2-10%). The artery provides branches to the posterior interventricular septum, interatrial septum, AVN, and penetrating bundle

of His (Sánchez-Quintana et al., 2001). In some patients, at the level of Koch's triangle the AVN arteryruns just beneath the endocardium near the ostium of the coronary sinus and septal isthmus (Fig. 2D). This may explain the possible risk of AVN artery coagulation during radiofrequency ablation in the slow pathway region, although a complete AV block is commonly a direct result of tissue injury to AVN (Jazayeri et al., 1992, Sánchez-Quintana et al., 2001). In a study of cadaveric hearts, Sánchez-Quintana et al., found that the mean distance of the artery to the endocardial surface at the base of Koch's triangle was 3.5 +/1.5 mm (Sánchez-Quintana et al., 2001).

3. *Cavotricuspid Isthmus (CTI) and Atrial Flutter*

Atrial flutter (AFL) can be categorized as being dependent on the cavotricuspid isthmus (CTI) or typical,and non-isthmus-dependent or atypical. The commonest type of atrial flutter is isthmus-dependent atrial flutter, in which the reentrant circuit is confined to the

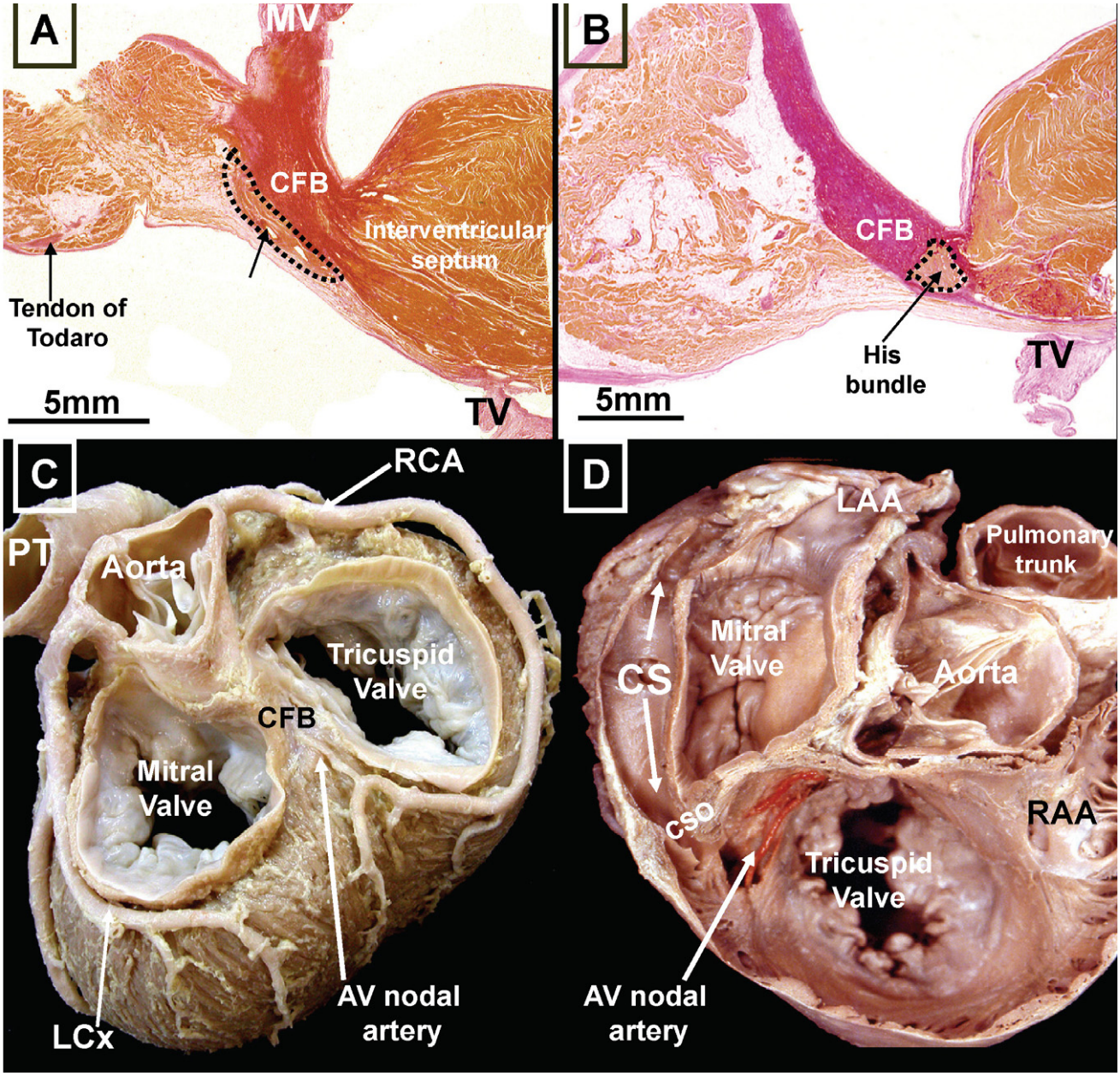

Figure 2. **A:** Sagittal histological section stained with elastic van Gieson through the compact part of the AV node (dashed black line) showing the nodal AV artery (arrow) in the middle of the node. **B:** Sagittal histological section stained with elastic van Gieson through the His bundle(dashed black line) in the thickness of the central fibrous body (CFB). **C:** The AV Nodal artery arises from the right coronary artery (RCA) and courses along the pyramidal space toward the central fibrous body. **D:** A window has been made through the inferior pyramidal space, showing the close relationship between the AV nodal artery and the coronary sinus orifice (CSO). MV: Mitral Valve; TV: Tricuspid Valve; CS: coronary sinus; LAA: Left Atrial Appendage; RAA: Right Atrial Appendage; LCx: Left Circumflex artery.

tricuspid annulus with the wave-front progressing either in a counterclockwise or clockwise direction across the CTI: the area between the IVC and the tricuspid valve (TV) (Fig. 3A). The CTI is the target of catheter-directed ablation procedures, the treatment of choice for AFL (Poty et al., 1996; Cauchemez et al., 1996). Autopsies, and angiographic and echocardiographic studies have shown that the anatomy of this structure (Figs. 3B and C) is highly variable (Cabrera et al., 1999; Cabrera et al., 2005; Heidbuchel et al., 2000): patients with a short and straight CTI require fewer radiofrequency ablation applications and

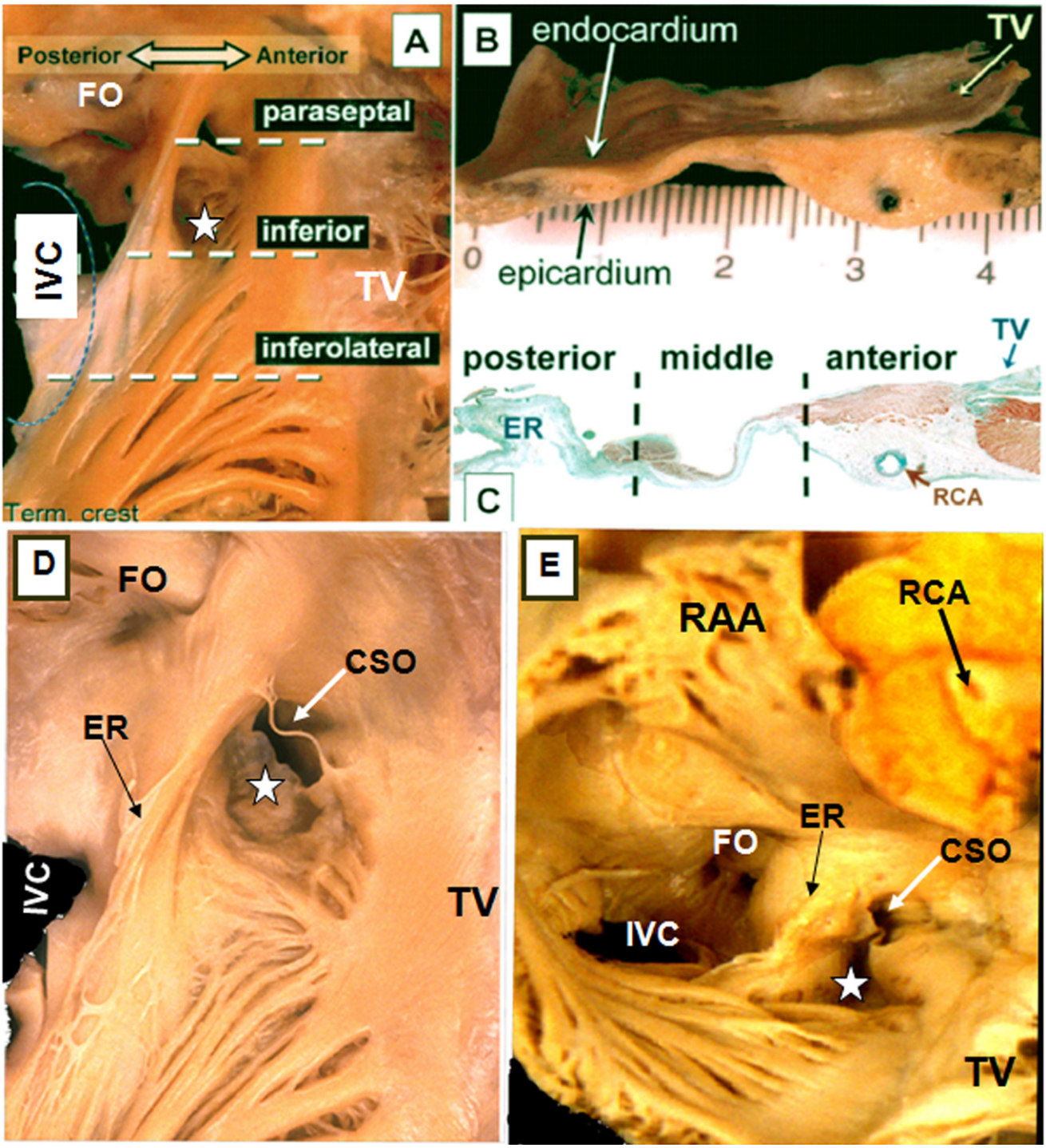

Figure 3. **A:** In this dissection, the endocardial surface of the right atrial isthmus is seen to show the three levels of the isthmus: paraseptal, inferior and inferolateral. Note the posterior recess or subthebesian recess (star) close to the inferior isthmus, and the distal ramifications of the terminal crest that feed into the inferolateral isthmus. **B:** The isthmus is seen in profile, and **C** shows a sagittal histological section stained with Masson´s trichrome stain. The anterior sector corresponds to the vestibule leading to the tricuspid valve (TV) and is related to the right coronary artery (RCA). The posterior sector is closest to the orifice of the inferior vena cava (IVC) and contains the Eustachian valve or ridge (ER) which is usually membranous. **D** and **E**: These panels show examples of variations in the morphology and depth of the subthebesian recess (star) in different specimens. IVC=inferior vena cava; TV=tricuspid valve; FO=fossa ovalis; CSO=Coronary sinus orifice; RAA: Right atrial appendage.

shorter X-ray exposure. Obstacles such as a large Eustachian ridge/valve (ER), a deep subthebesian recess (STR), and other pouch-like recesses may also lead to longer and more difficult ablation sessions (da Costa et al., 2004a) (Figs. 3 D and E). Cabrera et al. divided the CTI into three parallel levels (Cabrera et al., 1999; Cabrera et al., 2005). With the heart in attitudinal orientation, they identified and measured the lengths of three levels of the isthmus: paraseptal (24 ± 4 mm), inferior (19 ± 4 mm), and inferolateral (30 ± 3 mm). The paraseptal isthmus forms the base of Koch's triangle (Fig. 3A). The inferior isthmus, also known as the «central isthmus» owing to its location between the other two isthmuses, represents the optimal target for ablationsince this is the site where the IVC orifice is closest to the tricuspid valve insertion. It is also shown that most diameters are larger in patients with chronic AFL (larger RA) compared to paroxysmal AFL or control groups (Cabrera et al 2005; da Costa et al., 2004b). The dimensions of the CTI are highly variable. Anatomical studies with CT scan using image data obtained during different cardiac phases have shown that the CTI is longest at all three parallel levels during mid-ventricular systole (Saremi et al., 2008). In this phase the central isthmus length is greater than 30 mm in 32% of patients. The CTI varies in size during the cardiac cycle, becoming deeper with atrial contraction. The measurements have also shown a total of 40% variation in length during a single cardiac cycle. In around 28% of the population, a "hook-shaped" morphology is seen, showing a concave or pouch-like segment posteriorly (at the IVC side) and a flat vestibular part anteriorly.

4. *The Eustachian Ridge (ER) or valve*

The free border of the Eustachian valve continues as a tendon of Todaro that runs in the musculature of the Eustachian ridge (Fig. 3D and E). A large ER is an anatomic barrier and forms a line of fixed conduction block during typical atrial flutter. It has been demonstrated that in patients with a large ER, the paraseptal isthmus block can be obtained only after the complete ablation of the enlarged ER (Chang et al., 2007). Cabrera et al. (1999) demonstrated that 26% of their heart specimens had a thickened ER, with a mean thickness of 3.2 ± 0.8 mm. A thick ER > 4 mm is seen in 24% of the normal population studied with CT scans (Saremi et al., 2008). An angiographic study carried out by Heidbuchel et al. revealed an enlarged Eustachian valve in 24% of patients, with a consequent increase in the number of ablation pulse applications required for the achievement of a successful block (Heidbuchel et al., 2000).

5. *The Subthebesian recess (Sinus of Keith, SubEustachian sinus)*

The subthebesian recess (STR) is an extension of a pouch-like isthmus under the orifice of the CS (Figs. 3A, D and E). The presence of a large subthebesian recess or deep pouches is associated with significantly more RF applications as compared with straight isthmus (Malouf et al., 2004, Ho et al., 2002). Local radiofrequency delivery may be impaired by this structure because an area of limited blood flow results in delayed catheter tip cooling. In one angiographic study of the CTI, this pouch was observed in 47% of patients and had a mean depth of 4.3±2.1 mm (1.5 to 9.4) (Heidbuchel et al., 2000). CT scans in subthebesian normal populationhaverevealed a deep STR combined with a pouch-like (>5 mm) central isthmus in 45% of mid-diastolic phase images. This finding would be useful in preprocedural planning, where the presence of a large pouch would dictate a central approach to the ablation.

The Left Atrium (LA)

The LA is a very important structure for interventional cardiologists and is where subthebesian treatment of clinically important issues such as atrial fibrillation, atrial septal defects, mitral regurgitation, and left atrial thrombi may be approached. As with the RA, the LA possesses a venous component, a vestibule and an appendage (Anderson and Brown, 1996; Ho et al., 1999). The pulmonary venous component, with the venous orifices at each corner, is found posteriorly. The vestibular component surrounds the mitral orifice. The major part of the LA, including the pulmonary venous component, the vestibule, and the septal component, is smooth-walled (Fig. 4A). The left atrial appendage (LAA) is derived from the primitive atrium and has a rough, trabeculated surface (Figs. 4A and B). It is a potential site for subthebesian deposition of thrombi owing to its narrow neck with the LA. The atrial

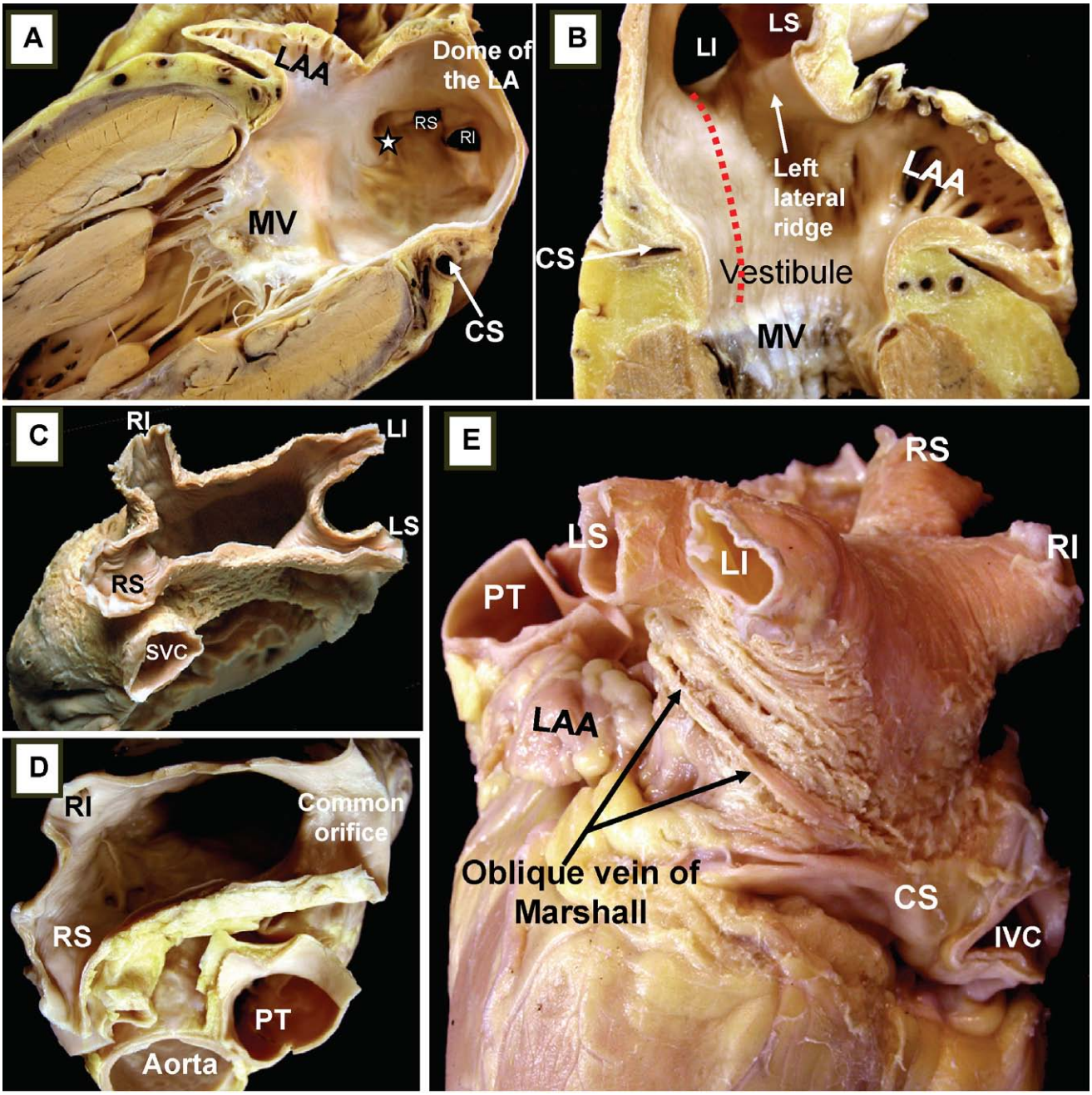

Figure 4. **A:** Parasagittal section of the left atrium (LA) and left ventricle to show that the smooth-walled venous component of the LA is the most extensive. The septal aspect of the LA shows the crescentic line of the free edge of the flap valve (star) against the rim of the fossa ovalis. The orifices of the right superior and inferior pulmonary veins (RS and RI) are adjacent to the plane of the septal aspect of the LA. **B:** Longitudinal section through the left atrial appendage (LAA) showing the orifices of the left pulmonary veins. Note the relationship between the left superior PV and the left lateral ridge. Note also the line connecting the inferior margin of the ostium of the left inferior PV to the mitral annulus, called the left atrial isthmus (dashed red line). **C** and **D:** Panel C shows the common ending and locations of PV and panel D shows a conjoined ostium on the left side, a common variant seen in up to 25% of cases. **E:** This is a dissection of the left atrium to show the myofibre arrangement in the subepicardium of the left lateral ridge, pulmonary veins, and the trajectory of the oblique vein of Marshall. Note that the vein of Marshall is in direct contact with the myocardium of the ridge. MV=mitral valve; SVC: Superior vena cava; LAA: Left atrial appendage; PT=Pulmonary trunk; CS=coronary sinus; RS=right superior pulmonary vein; RI=right inferior pulmonary vein; IVC: Inferior vena cava; LI=left inferior pulmonary vein; LS=left superior pulmonary vein.

appendage of the left atrium is considerably smaller and tends to have a tubular shape with one or several bends resembling a little finger. The rough zone of the left atrium is mainly confined to its appendage. A complicated network of fine muscular ridges lines the endocardial aspect (Figs. 4A and B). In between the ridges, the wall is parchment thin. The anterior wall just behind the aorta is usually thin and vulnerable to injury. The superior wall, or dome, is thickest, measuring 3.5 to 6.5 mm (Ho et al., 1999).

1. *The Pulmonary Veins and Atrial Fibrillation (AF)*

AF is the most common sustained cardiac arrhythmia and is characterized by uncoordinated contraction of the atrium. Although different mechanisms of atrial fibrillation exist, it is well established that the myocardial sleeves of the pulmonary veins (PV), especially the superior veins, are crucial sources of triggers that initiate AF (Haissaguerre et al., 1998). Cardiac ablation is performed in symptomatic AF, which is refractory to at least one Class 1 or 3 antiarrhythmic medications. In elderly patients, myocardial perforation and thromboembolic complications of the ablation are more prevalent. Furthermore, patients with larger LA size and longer AF duration typically experience a higher incidence of AF recurrence (Haissaguerre et al., 1998). Previously, the most common ablation strategy was electrical isolation of the PVs by creating circumferential ablation lines around the individual or bilateral PV ostia. The lines are guided by fluoroscopy, 3D electroanatomical mapping (Pappone et al., 2001, Takahashi et al., 2002) or intracardiac echocardiography (ICE) (Marrouche et al., 2003). However, the focus of ablation strategies shifted from the PV to the atrial tissue located in the antrum due to the fact that many non-PV trigger points for AF are located in the antrum rather than the PV and that RF delivery may cause PV stenosis (Ouyang et al., 2004). In antrum ablation, the most common sites are the LA «roof», connecting the superior aspects of the left and right upper PV isolation lesions, the region of tissue between the mitral valve, and the left inferior PV (the mitral isthmus) (Ouyang et al., 2004). These techniques result in success rates of more than 90% with long-term success rates ranging from 60 to 90 % in patients with paroxysmal AF but lower rates in those with chronic AF ((Ouyang et al., 2004). Vagal stimulation shortens the atrial effective refractory period that facilitates the initiation and maintenance of AF. Adding the LA ganglion plexus to other ablation targets may improve the success of ablationin patients undergoing circumferential PV ablation for paroxysmal AF (Pappone et al., 2004). Normal pulmonary vein (PV) anatomy consists of two right-sided and two left-sided PVs with separate ostia (Fig. 4C). However, in anatomical studies with multidetector CT scanners (MDCT) it has been demonstrated that the anatomy of the LA and PVs is commonly variable (Schwartzman et al., 2003) (Fig. 4D). The PV ostia are ellipsoid with a longer superior-inferior dimension. The right superior PV is located close to the SVC or RA, and the right inferior PV projects horizontally. The left superior PV is close to the LAA and the left inferior PV courses near the descending aorta. The eins are larger in AF versus non-AF patients, men versus women, and persistent versus paroxysmal patterns. The PV trunk is defined as the distance from the ostium to the first-order branch. The superior pulmonary vein ostia are larger (19-20 mm) than the inferior pulmonary vein ostia (16-17 mm) (Cronin et al., 2004). The superior pulmonary veins tend to have a longer trunk (21.6 ± 7.5 mm) than the inferior PVs (14.0 ± 6.2 mm) (Cronin et al., 2004). It is important to note the ostial diameters of each vein and the length to the first-order branch. These diameters influence the selection of the circular catheter size used.

Common anomalies include a conjoined (common) left or right pulmonary vein in 25% of individuals (Cronin et al., 2004). A conjoined PV is seen more frequently on the left than the right side (Maron et al., 2004). Supernumerary veins are also frequent. The most common is a separate right middle pulmonary vein, which drains the middle lobe of the lung (Jongbloed et al., 2005). One or two middle lobe vein ostia can be seen in 26% of patients (Maron et al., 2004). The ostial diameter of the right middle pulmonary vein is smaller than that of the other veins (mean, 9.9 ± 1.9 mm). The ectopic focus originating from the right middle PV could initiate AF, which is cured by catheter ablation of the right middle PV. In some patients, there is a supernumerary PV that shows an aberrant insertion, with a perpendicular position in relation to the LA posterior wall. The supernumerary branch usually drains the upper lobe of the right lung and characteristically passes behind the bronchus intermedius. The absence of one PV requires careful examination ofthe whole intra-thoracic venous system since it may be associated with partial anomalous venous return. The calibre of the PVs gradually increases as they approach the left atrium. However, the calibre of the left inferior pulmonary vein may decrease as it enters the LA and this should not be mistaken for stenosis (Tsao et al., 2001).

2. *Left Atrial Isthmus and Atrial Fibrillation*

In patients with atrial fibrillation (AF), the success rate of catheter ablation depends on adequate electrical isolation by performing linear ablation lesions. However, a recurrence of atrial arrhythmias is not uncommon, particularly in the left atrial isthmus, the area between the orifice of the left inferior pulmonary vein, and the posteroinferior mitral annulus (Jais et al., 2004) (Fig. 4B). The left atrial isthmus varied in length, running from 17 to 51 mm (Becker, 2004). CT can accurately demonstrate the boundaries of this area including the exact location of the mitral valve, the coronary sinus, circumflex artery and the great cardiac vein and their anatomic variants (Becker, 2004).

3. *The Oblique Vein of Marshall and Persistent Left Superior Vena Cava (SVC)*

Non-PV triggers initiating AF can be identified in up to one third of unselected patients referred for catheter ablation for paroxysmal AF (Shah et al., 2003). The sites of origin for non-PV atrial triggers include the posterior wall of the LA, SVC, crista terminalis, fossa ovalis, coronary sinus, behind the Eustachian ridge, along the ligament of Marshall, and adjacent to the atrioventricular valve annuli. The oblique vein of Marshall, located between the LAA and the left upper and lower pulmonary veins, runs inferiorly along the inferior atrial wall to join the coronary sinus (CS) (Fig. 4E) approximately 3 cm from its ostium. In most hearts (70%), the oblique vein or ligament of Marshall is <3 mm from the endocardium of the left lateral ridge and has muscular connections to the left PVs (Cabrera et al., 2008). The remnant of the oblique vein can be detected in coronary CT studies. It remains patent as an isolated malformation, the persistent left SVC draining into the CS in 0.3% of the normal population, and can be the source of AF (Hsu et al., 2004).

Important structures in the neighborhood of the heart

1. *Relationship between the Oesophagus and LA*

Due to the close proximity of the oesophagus to the posterior wall of the LA (Sánchez-Quintana et al., 2005b) (Fig. 5A and B), ablation procedures involving this region of the LA may cause oesophageal damage and result in the formation of an atrial oesophageal fistula (Cummings et al., 2006). Multidetector CT scanner (MDCT) valuable tools for showing the relationship of the atrial wall and the oesophagus and the descending aorta prior to the ablation procedure (Lemola et al., 2004). However, peristalsis and dynamic movement of the oesophagus during the procedure can result in discordance between the preprocedure and intraprocedure anatomy.

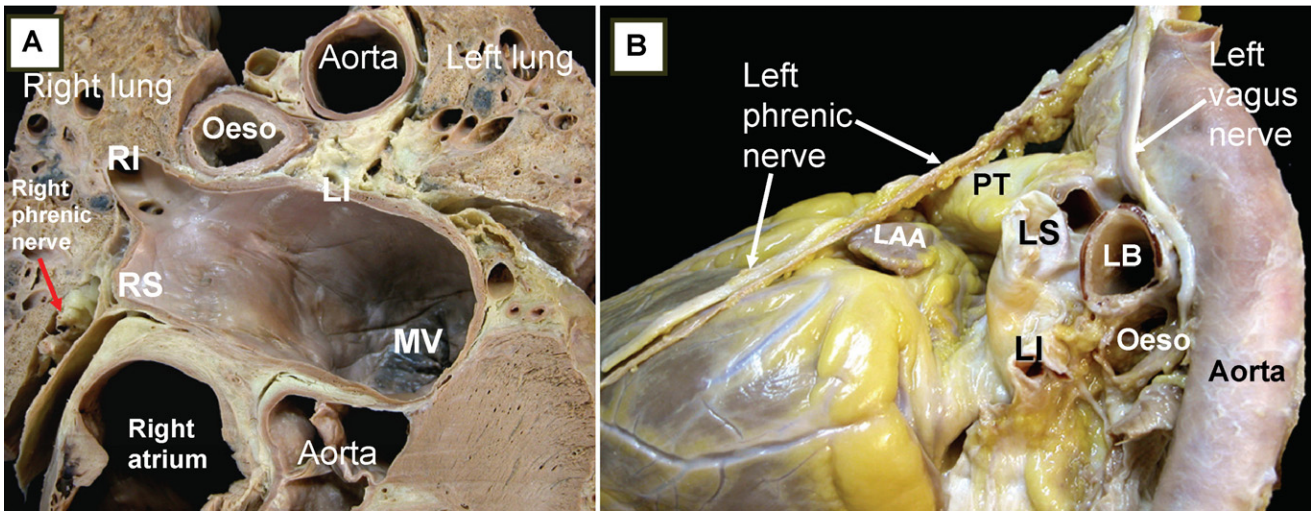

Figure 5. **A:** An overview of a transthoracic section through a cadaver showing the locations of the oesophagus, the descending aorta and the right phrenic nerve. Note the minimal distance between the endocardial surface of the left atrium and the oesophagus or the right phrenic nerve relative to the right superior pulmonary vein (RS). **B:** Dissection of the left phrenic nerve, which descends onto the fibrous pericardium anterior and lateral to the aortic arch, alongside the distal part of pulmonary trunk, left atrial appendage (LAA), and the lateral wall of the left ventricle, to penetrate the left part of the diaphragm. MV: Mitral valve; Oeso: Oesophagus; LB= Left bronchus; RI=Right inferior pulmonary vein; LS=Left superior pulmonary vein; LI=Left inferior pulmonary vein.

2. *The Phrenic Nerves*

The phrenic nerves lie along the lateral mediastinum and run from the thoracic inlet to the diaphragm (Sánchez-Quintana et al., 2005c). Phrenic nerve injury results from direct thermal injury, usually to the right phrenic nerve, which is located near the right superior PV and the SVC (Sánchez-Quintana et al., 2005c; Sacher et al., 2006) (Fig. 5A). Less frequently, ablation within the LA appendage can result in left phrenic nerve damage (Sánchez-Quintana et al., 2009) (Fig. 5B). MDCT coronary angiography can demonstrate the left phrenic neurovascular bundle as it passes over the LV pericardium in 74% of the studies (Matsumoto et al., 2007). However, it is difficult to image the right phrenic nerve. In some high-quality images, the right phrenic nerve can be seen as a mildly enhancing the extrapericardial structure lateral to the SVC and anterior to the right superior pulmonary vein.

References

Anderson KR, Ho SY, Anderson RH (1979) Location and vascular supply of sinus node in human heart. *Br Heart J*, 41: 28-32.

Anderson RH, Brown NA (1996) The anatomy of the heart revisited. *Anat Rec*, 246: 1-7.

Anderson RH, Ho HY, Becker AE (2000) Anatomy of the human atrioventricular junctions revisited. *Anat Rec*, 260: 81-91.

Becker AE (2004) Left atrial isthmus. Anatomic aspects relevant for linear catheter ablation procedures in humans. *J Cardiovasc Electrophysiol*, 15: 809-812.

Cabrera JA, Ho SY, Climent V, Sánchez-Quintana D (2008) The architecture of the left lateral atrial wall: a particular anatomic region with implications for ablation of atrial fibrillation. *Eur Heart J*, 29: 356-362.

Cabrera JA, Sánchez-Quintana D, Farre J, Rubio JM, Ho SY (2005) The inferior right atrial isthmus: further architectural insights for current and coming ablation technologies. *J Cardiovasc Electrophysiol*, 16: 409-410.

Cabrera JA, Sánchez-Quintana D, Ho SY, Medina A, Wanguemert F, Gross E, Grillo J, Hernandez E, Anderson RH (1999) Angiographic anatomy of the inferior right atrial isthmus in patients with and without history of common atrial flutter. *Circulation*, 99: 3017-3023.

Cauchemez B, Haïssaguerre M, Fischer B, Thomas O, Clementy J, Coumel P (1996) Electrophysiological effects of catheter ablation of inferior vena cava-tricuspid annulus isthmus in common atrial flutter. *Circulation*, 93: 284-294.

Cronin P, Sneider MB, Kazerooni EA, Kelly AM, Scharf C, Oral H, Morady F (2004) MDCT of the left atrium and pulmonary veins in planning radiofrequency ablation for atrial fibrillation: A how-to guide. *AJR Am J Roentgenol*, 183: 767-778.

Cummings JE, Schweikert RA, Saliba WI, Burkhardt JD, Kilikaslan F, Saad E, Natale A (2006) Brief communication: atrialesophageal fistulas after radiofrequency ablation. *Ann Intern Med*, 144: 572-574.

Chang SL, Tai CT, Lin YJ, Ong MG, Wongcharoen W, Lo LW, Chang SH, Hsieh MH, Chen SA (2007) The electroanatomic characteristics of the cavotricuspid isthmus: implications for the catheter ablation of atrial flutter. *J Cardiovasc Electrophysiol*, 18: 18-22.

Chiu I, Hung CR, How SW, Chen MR (1989) Is the sinus node visible grossly? A histological study of normal hearts. *Int J Cardiol*, 22: 83-87.

Da Costa A, Faure E, Thevenin J, Messier M, Bernard S, Abdel K, Robin C, Romeyer C, Isaaz K (2004a) Effect of isthmus anatomy and ablation catheter on radiofrequency catheter ablation of the cavotricuspid isthmus. *Circulation*, 110: 1030-1035.

Da Costa A, Mourot S, Romeyer-Bouchard C, Thévenin J, Samuel B, Kihel A, Isaaz K (2004b) Anatomic and electrophysiological differences between chronic and paroxysmal forms of common atrial flutter and comparison with controls. *Pacing Clin Electrophysiol*, 27: 1202-1211.

Haissaguerre M, Jais P, Shah DC, Takahashi A, Hocini M, Quiniou G, Garrigue S, Le Mouroux A, Le Métayer P, Clémenty J (1998) Spontaneous initiation of AF by ectopic beats originating in the pulmonary veins. *N Engl J Med*, 339: 659-666.

Heidbuchel H, Willems R, Van Rensburg H, Adams J, Ector H, Van De Werf F (2000) Right atrial angiographic evaluation of the posterior isthmus: relevance for ablation of typical atrial flutter. *Circulation*, 101: 2178-2184.

Ho SY, Anderson RH, Sanchez-Quintana D (2002) Atrial structure and fibres: morphologic bases of atrial conduction. *Cardiovasc Res*, 54: 325-336.

Ho SY, Anderson RH (2000) How constant anatomically is the tendon of Todaro as a marker for the triangle of Koch? *J Cardiovasc Electrophysiol*, 11: 83-89.

Ho SY, Sánchez-Quintana D, Cabrera JA, Anderson RH (1999) Anatomy of the left atrium: implications for radiofrequency ablation of atrial fibrillation. *J Cardiovasc Electrophysiol*, 10: 1525-1533.

Hsu LF, Jais P, Keane D, Wharton JM, Deisenhofer I, Hocini M, Shah DC, Sanders P, Scavée C, Weerasooriya R, Clémenty J, Haïssaguerre M (2004) Atrial fibrillation originating from persistent left superior vena cava. *Circulation*, 109: 828-832.

Inoue S, Shinohara F, Niitani H, Gotoh K (1986) A new method for the histological study of aging changes in the sinoatrial node. *Jpn Heart J*, 27: 653-660.

Jais P, Hocini M, Hsu LF, Sanders P, Scavee C, Weerasooriya R, Macle L, Raybaud F, Garrigue S, Shah DC, Le Metayer P, Clémenty J, Haïssaguerre M (2004) Technique and results of linear ablation at the mitral isthmus. *Circulation*, 110: 2996-3002.

Jazayeri MR, Hempe SL, Sra JS, Dhala AA, Blanck Z, Deshpande SS, Avitall B, Krum DP, Gilbert CJ, Akhtar M (1992) Selective transcatheter ablation of the fast and slow pathways using radiofrequency energy in patients with atrioventricular nodal re-entrant tachycardia. *Circulation*, 85: 1318-1328.

Jongbloed MR, Bax JJ, Lamb HJ, Dirksen MS, Zeppenfeld K, Van Der Wall EE, De Roos A, Schalij MJ (2005) Multislice computed tomography versus intracardiac

echocardiography to evaluate the pulmonary veins before radiofrequency catheter ablation of atrial fibrillation: a head-to-head comparison. *J Am Coll Cardiol*, 45: 343-350.

Lemola K, Sneider M, Desjardins B, Case I, Han J, Good E, Tamirisa K, Tsemo A, Chugh A, Bogun F, Pelosi F JR, Kazerooni E, Morady F, Oral H (2004) Computed tomographic analysis of the anatomy of the left atrium and the esophagus: implications for left atrial catheter ablation. *Circulation*, 110: 3655-3660.

Malouf JF, Edwards WD, Tajik AJ, Seward JB (2004) Functional anatomy of the heart. In: Fuster V, Alexander RW, O'Rourke RA et al (eds): *The Heart*, 11th ed. McGraw-Hill, New York, pp 75-83.

Man KC, Knight B, Tse HF, Pelosi F, Michaud GF, Flemming M, STRICKBERGER SA, MORADY F (2000) Radiofrequency catheter ablation of inappropriate sinus tachycardia guided by activation mapping. *J Am Coll Cardiol*, 35: 451-457.

Marom EM, Herndon JE, Kim YH, McAdams HP (2004) Variations in pulmonary venous drainage to the left atrium: implications for radiofrequency ablation. *Radiology*, 230: 824-829.

Marrouche NF, Martin DO, Wazni O, Gillinov AM, Klein A, Bhargava M, Saad E, Bash D, Yamada H, Jaber W, Schweikert R, Tchou P, Abdul-Karim A, Saliba W, Natale A (2003) Phased-array intracardiac echocardiography monitoring during pulmonary vein isolation in patients with atrial fibrillation: impact on outcome and complications. *Circulation*, 107: 2710-2716.

Matsumoto Y, Krishnan S, Fowler SJ, Saremi F, Kondo T, Ahsan C, Narula J, Gurudevan S (2007) Detection of phrenic nerves and their relation to cardiac anatomy using 64-slice multidetector computed tomography. *Am J Cardiol*, 100: 133-137.

Matsuyama TA, Inoue S, Kobayashi, Sakai T, Saito T, Katagiri T, Ota H (2004) Anatomical diversity and age-related histological changes in the human right atrial posterolateral wall. *Europace*, 6: 307-315.

Mizumaki K, Fujiki A, Nagasawa H, Nishida K, Sakabe M, Sakurai K, Inoue H (2002) Relation between transverse conduction capability and the anatomy of the crista terminalis in patients with atrial flutter and atrial fibrillation: analysis by intracardiac echocardiography. *Circ J*, 66: 1113-1118.

Ouyang F, Bansch D, Ernst S, Schaumann A, Hachiya H, Chen M, Chun J, Falk P, Khanedani A, Antz M, Kuck KH (2004) Complete isolation of left atrium surrounding the pulmonary veins: new insights from the double-Lasso technique in paroxysmal atrial fibrillation. *Circulation*, 110: 2090-2096.

Pappone C, Oreto G, Rosanio S, Vicedomini G, Tocchi M, Gugliotta F, Salvati A, Dicandia C, Calabrò MP, Mazzone P, Ficarra E, Di Gioia C, Gulletta S, Nardi S, Santinelli V, Benussi S, Alfieri O (2001) Atrial electroanatomic remodeling after circumferential radiofrequency pulmonary vein ablation: efficacy of an anatomic approach in a large cohort of patients with atrial fibrillation. *Circulation*, 104: 2539-2544.

Pappone C, Santinelli V, Manguso F, Vicedomini G, Gugliotta F, Augello G, Mazzone P, Tortoriello V, Landoni G, Zangrillo A, Lang C, Tomita T, Mesas C, Mastella E, Alfieri O (2004) Pulmonary vein denervation enhances long-term benefit after circumferential ablation for paroxysmal atrial fibrillation. *Circulation*, 109: 327-334.

Poty H, Saoudi N, Nair M, Anselme F, Letac B (1996) Radiofrequency catheter ablation of atrial flutter. Further insights into the various types of isthmus block: application to ablation during sinus rhythm. *Circulation*, 94: 3204-3213.

Sacher F, Monahan KH, Thomas SP, Davidson N, Adragao P, Sanders P, Hocini M, Takahashi Y, Rotter M, Rostock T, Hsu LF, Clémenty J, Haïssaguerre M, Ross DL, Packer DL, Jaïs P (2006) Phrenic nerve injury after atrial fibrillation catheter ablation: characterization and outcome in a multicenter study. *J Am Coll Cardiol*, 47: 2498-2503.

Sánchez-Quintana D, Ho SY (2003) Anatomy of cardiac nodes and atrioventricular specialized conduction system. Rev Esp Cardiol, 56: 1085-1092.

Sánchez-Quintana D, Ho SY, Cabrera JA, Farre J, Anderson RH (2001) Topographic anatomy of the inferior pyramidal space: relevance to radiofrequency catheter ablation. *J Cardiovasc Electrophysiol*, 12: 210-217.

Sánchez-Quintana D, Anderson RH, Cabrera JA, Climent V, Martin R, Farré J, Ho SY (2002) The terminal crest: morphological features relevant to electrophysiology. *Heart*, 88: 406-411.

Sánchez-Quintana D, Cabrera JA, Farré J, Climent V, Anderson RH, Ho SY (2005a) Sinus node revisited in the era of electroanatomical mapping and catheter ablation. *Heart*, 91: 189-194.

Sánchez-Quintana D, Cabrera JA, Climent V, Farré J, Mendonça MC, Ho SY (2005b) Anatomic relations between the esophagus and left atrium and relevance for ablation of atrial fibrillation. *Circulation*, 112: 1400-1405.

Sánchez-Quintana D, Cabrera JA, Climent V, Climent V, Farré J, Weiglein A, Ho SY (2005c) How close are the phrenic nerves to cardiac structures? Implications for cardiac interventionalists. *J Cardiovasc Electrophysiol*, 16: 309-313.

Sánchez-Quintana D, Ho SY, Climent V, Murillo M, Cabrera JA (2009) Anatomic evaluation of the left phrenic nerve relevant to epicardial and endocardial catheter ablation: Implications for phrenic nerve injury. *Heart Rhythm*, 6: 764-768.

Saremi F, Pourzand L, Krishnan S, Ashikyan O, Gurudevan SV, Narula J, Kaushal K, Raney A (2008) Right atrial cavotricuspid isthmus: anatomic characterization with multi-detector row CT. *Radiology*, 247: 658-668.

Schwartzman D, Lacomis J, Wigginton WG (2003) Characterization of left atrium and distal pulmonary vein morphology using multidimensional computed tomography. *J Am Coll Cardiol*, 41: 1349-1357.

Shah D, Haissaguerre M, Jais P, Hocini M (2003) Non-pulmonary vein foci: do they exist? *Pacing Clin Electrophysiol*, 26: 1631-1635.

Takahashi A, Iesaka Y, Takahashi Y, Takahashi R, Kobayashi K, Takagi K, Kuboyama O, Nishimori T, Takei H, Amemiya H, Fujiwara H, Hiraoka M (2002) Electrical connections between pulmonary veins: implication for ostial ablation of pulmonary veins in patients with paroxysmal atrial fibrillation. *Circulation*, 105: 2998-3003.

Tsao HM, Wu MH, Yu WC, Tai CT, Lin YK, Hsieh MH, Ding YA, Chang MS, Chen SA (2001) Role of right middle pulmonary vein in patients with paroxysmal atrial fibrillation. *J Cardiovasc Electrophysiol*, 12: 1353-1357.